Contents lists available at ScienceDirect

Arabian Journal of Chemistry

journal homepage: www.ksu.edu.sa

Original article

Design, synthesis, and evaluation of novel 3-(piperazin-1-yl) propan-2-ol-modified carbazole derivatives targeting the bacterial membrane

Si-Yue Ma [a,1], Ying-Guo Ding [a,b,1], Xin-Xin Tuo [a], Guo-Qing Wang [a], Hong-Wu Liu [a], Jiao Meng [a], Tai-Hong Zhang [a], Li-Wei Liu [a], Pu-Ying Qi [a], Xiang Zhou [a,*], Song Yang [a,*]

[a] State Key Laboratory of Green Pesticide, Key Laboratory of Green Pesticide and Agricultural Bioengineering, Ministry of Education, Center for R&D of Fine Chemicals of Guizhou University, Guiyang 550025, China
[b] Anlong Jiayou Shuyuan High School, Anlong 552400, China

ARTICLE INFO

Keywords:
Carbazole derivatives
Antibacterial activity
Cell membrane
Plant bacterial diseases

ABSTRACT

Grain of high yield and quality is needed worldwide due to the needs of a rapidly increasing human population. However, diseases caused by some stubborn types of phytopathogenic bacteria can limit the health and yields of crops. Even worse, conventional commercial bactericides have limited efficacy against such diseases. Therefore, exploring some efficacious bactericidal alternatives is urgently needed. In this work, a new type of 3-(piperazin-1-yl)propan-2-ol modified carbazole derivatives was synthesized and assessed for their bactericidal activity. Among them, compound **B_{16}** was the optimal active molecule, giving the EC_{50} values of 3.11 (*Xanthomonas oryzae* pv. *oryzae*), 3.20 (*Xanthomonas axonopodis* pv. *citri*) and 3.54 μg/mL (*Pseudomonas syringae* pv. *actinidiae*). Pot experiments revealed compound **B_{16}** to be able to control rice bacterial leaf blight. Some biochemical assays illustrated that our designed compounds could destroy the integrality of bacterial cell membranes and thereby leading to leaking the intracellular protein. These findings may be regard as a reference for the design of novel membrane-targeting antimicrobial agents for managing stubborn plant bacterial diseases.

1. Introduction

Grain of high yield and quality is needed worldwide due to the needs of a rapidly increasing human population (Zeng et al., 2017; Benchlih et al., 2023; Xiang et al., 2023). However, diseases caused by some stubborn types of phytopathogenic bacteria can limit the health and yields of crops (Yang et al., 2023; Ali et al., 2022; Ma et al., 2022). For instance, *Xanthomonas oryzae* pv. *oryzae* (*Xoo*), *Xanthomonas axonopodis* pv. *citri* (*Xac*), and *Pseudomonas syringae* pv. *actinidiae* (*Psa*) can destroy the plants and products of rice, citrus fruits, and kiwifruit (Qi et al., 2023a; Lu et al., 2023). The application of agrochemicals is considered to be the most effective measure to manage these bacterial diseases in plants (Xiao et al., 2023).

However, long-term use of traditional bactericidal drugs has led grievous resistance, for example, streptomycin sulfate (Lyu et al., 2019). The emergence of resistant phytopathogens means that existing products must be used more effectively and new products must be developed. Notably, targeting the cell membrane of bacteria has become an attractive strategy to kill bacteria (Jin et al., 2020; Naclerio and Sintim, 2020; Cauz et al., 2019).

Products derived from natural sources have been widely used to develop new pesticides and medicines (Ran et al., 2023; Ji et al., 2022). Their diverse structure, abundance resources, and environmental friendliness has enabled the development of pesticides for controlling insects, weeds, and microbes (Hasheminejad et al., 2019; Fang et al., 2022).

An increasing number of naturally available carbazole derivatives (Fig. 1) has been shown to have antibacterial (Ashok et al., 2016), antifungal (Merzouki et al., 2023), antiviral (Yang et al., 2019), and anticancer properties (Issa et al., 2019) in human medicine. However, use of simple carbazole-based derivatives to counteract phytopathogenic bacteria in farming is rare. Numerous studies have revealed the importance of carbazoles targeting the cell membrane, which have promising prospects for the discovery of new antibacterial agents for

* Corresponding authors.
E-mail addresses: xiangzhou@gzu.edu.cn (X. Zhou), syang@gzu.edu.cn (S. Yang).
[1] The two authors contributed equally to this work.

https://doi.org/10.1016/j.arabjc.2024.105850
Received 9 March 2024; Accepted 29 May 2024
Available online 6 June 2024

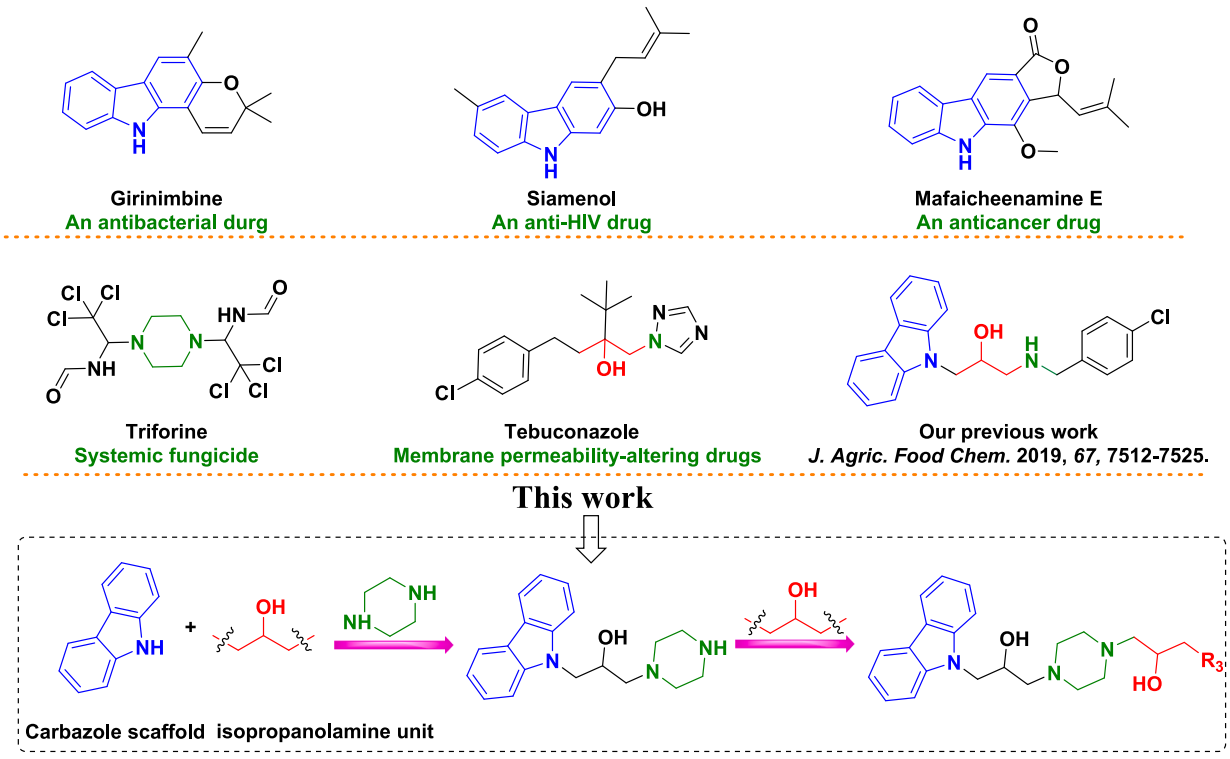

Fig. 1. Some carbazole, piperazine, and isopropanolamine structures and the design strategy of title molecules.

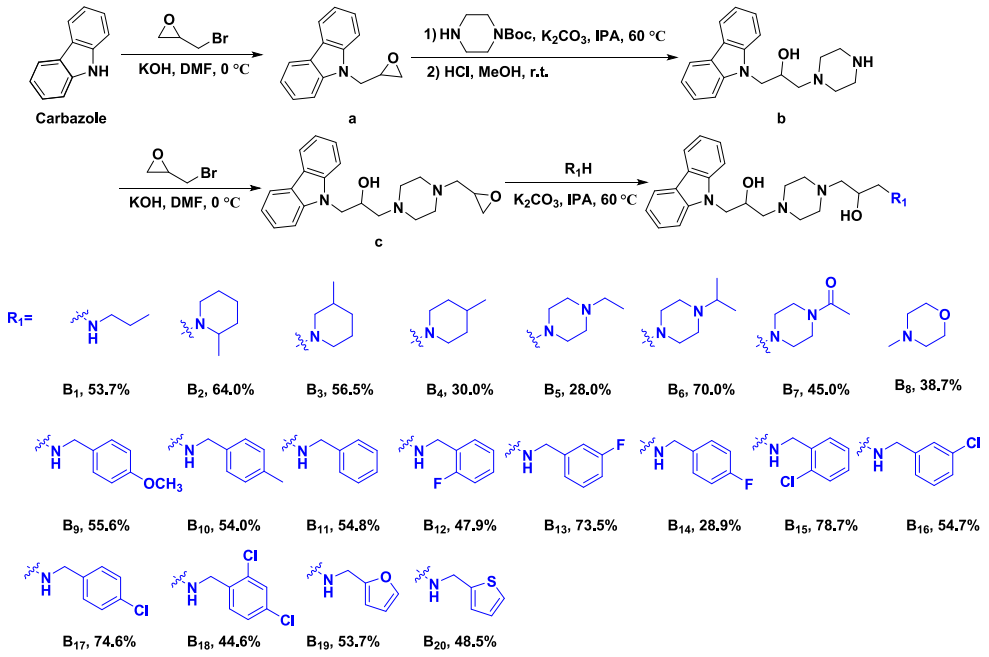

Fig. 2. Synthesis procedure for title molecules B_1–B_{20}.

managing plant diseases caused by bacterial infection (Hurley et al., 2015; Lin et al., 2020). Some carbazole derivatives reported by our research team have been shown to have promising skeletons for the discovery of novel agents to manage diverse bacterial diseases in plants (Huang et al., 2021; Zhao et al., 2019a). Advanced literature and our previous work showed that carbazole core had the ability to target bacterial cell membranes. Hence, carbazoles have attracted researchers' attention for the discovery of new cell membrane-targeting bactericides. (Lin et al., 2020, Xue et al., 2021; Gerits et al., 2016) Meanwhile, Shaquiquzzaman and colleagues (Shaquiquzzaman et al., 2015) and Vignaroli (Vignaroli et al., 2017) stated that piperazine and isopropanolamine moieties displayed antibacterial (Zeng et al., 2023a), antifungal (Chen et al., 2020), anticancer (Keskin et al., 2016), anti-inflammatory (Jain et al., 2020), and antiviral activities (Aggarwal et al., 2017), as well as being soluble in water. In addition, the piperazine and isopropanolamine moieties were further discovered to potentially disrupt membrane integrity and function by forming a strong binding affinity toward bacterial membranes (Zhou et al., 2023; Zeng

et al., 2023a). Thus, engineering new derivatives of carbazoles by introducing piperazine and isopropanolamine moieties may provide new perspectives for discovering novel antibacterial agents.Fig. 2..

In this work, in order to probe more efficacious antibacterial active molecules, novel types of 3-(piperazin-1-yl)propan-2-ol-based carbazoles were elaborately prepared. Furthermore, the *in vitro* and *in vivo* antibacterial potency of all title molecules against three intractable pathogenic strains (*Xoo*, *Xac*, and *Psa*) were evaluated *via* turbidimetric tests and pot experiments. The potential antibacterial mechanisms of designed molecules were studied by using scanning electron microscopy (SEM), electrical conductivity, and fluorescence staining.

2. Materials and methods

2.1. Instruments and chemicals

Nuclear magnetic resonance (NMR) spectroscopy of intermediates and target compounds was done using an ECX 500 system or Biospin AG-400 setup. High-resolution mass spectrometry (HRMS) was done using a Q-Exactive Orbitrap system. Methanol was used as the solvent for liquid chromatography-mass spectrometry.

TEM images were imaged using an FEI Talos F200C electron microscope (FEI) with a voltage of 200 kV. The molecular ζ-potential was assayed by the DelsaNanoC analyzer. The *in vitro* antibacterial evaluation was expressed as OD_{595} value, and monitored by using Cytation™ 5 multi-mode readers. Finally, cell membrane permeability experiment was conducted by a DDS-307 electrical conductivity analyzer.

2.2. General experimental procedure

In vitro and *in vivo* bioassays towards the pathogenic bacteria, as well as cell membrane-permeability studies, and morphological study, were conducted according to methods described in our previous works (Li et al., 2023; Qi et al., 2023b; Shao et al., 2023; Chu et al., 2023; Wang et al., 2022). The wild-type (WT) *Xanthomonas oryzae* pv. *oryzae* (*Xoo*) strain ZJ173 comes from Nanjing Agricultural University which was kindly provided by Ming-Guo Zhou.

2.3. Propidium iodide (PI) staining assay

We wished to evaluate the permeability and integrity of *Xoo* cells stimulated by our designed molecules (Perrine-Walker and Le, 2020; Rego et al., 2022). PI staining was carried out and compound **B_{16}** (half-maximal effective concentration (EC_{50}) = 3.11 μg/mL against *Xoo* cells) was selected as the treatment molecule. In detail, *Xoo* cells were cultured at logarithmic phase [optical density at 595 nm (OD_{595}) = 0.6–0.8] and adjusted to 0.2 (OD_{595}). Then, *Xoo* cells were treated with molecule **B_{16}** (0, 6.22, 12.44, or 24.88 μg/mL) for 14 h in a shaker (28 °C, 180 rpm). Furthermore, *Xoo* cells were collected by centrifugation (8000 × *g*, 2 min, 4 °C) and resuspended in 10 mM of phosphate-buffered saline (pH = 7.2). Finally, 100 μL of the treated *Xoo* cultures was stained by PI solution (20 μg/mL, 10 μL) for 20 min, and then the images were collected on a fluorescence spectrophotometer with Olympus BX53 microscope (Olympus, Tokyo, Japan).

2.4. Detection of intracellular protein in Xoo cells

The protein concentration within *Xoo* cells was verified by SDS-PAGE (Yang et al., 2021). Briefly, samples were treated with compound **B_{16}** (0, 0.78, 1.56, 3.11, and 6.22 μg/mL) as described in section 2.3. After incubation for 14 h, treated *Xoo* cells were collected and lysed *via* sonication (power: 35 %; ultrasound: 5 s; interval: 5 s) for 30 min on an ice bath. Total intracellular proteins were obtained by centrifugation (10000 rpm, 10 min, room temperature) to remove *Xoo* cell debris. Furthermore, the protein concentration was measured by the Bradford assay and diluted to 20 times with PBS. Finally, the protein content of *Xoo* cells in the supernatant of each sample was analyzed by SDS-PAGE.

2.5. Compound B_{16} interacts with the DNA of Xoo

According to the previously experimental method (Zhao et al., 2019b). DNA of *Xoo* a was extracted using the TIANamp Bacteria DNA Kit, and the concentration was further measured by a UV–1900 spectrophotometer (Shimadzu Co., Japan) to be a value of 9.38×10^{-8} mol/L (ξ_{260} = 6600 L mol^{-1} cm^{-1}). Furthermore, compound **B_{16}** diluted in Tris-HCl buffer solution (50 mM, pH 7.4) to yield a final concentration of 1×10^{-8} mol/L. Following the addition of the different dosages of DNA at room temperature for 20 min. The fluorescence spectra of mixture were recorded using an PTI QuantaMaster 8000 fluorescence spectrophotometer (Horiba Scientific, Canada), equipped with a 1.0 cm quartz cell. Both the excitation and emission slit widths were set to 5 nm, with an excitation wavelength of 363 nm.

2.6. Pathogenicity assay

According to our previous work (Zeng et al., 2023b; Jin et al., 2020), *Xoo* cells (OD_{595} = 0.1) were treated with compound **B_{16}** (0.78, 1.56, 3.11, and 6.22 μg/mL) for 21 h; an equal volume of DMSO was used as the negative control. All treated *Xoo* cells were centrifuged and resuspended using sterile water to ensure OD_{595} = 0.5. Thereafter, the resuspended *Xoo* solutions were treated on rice leaves using the leaf-cutting method. All treatments were repeated thrice followed by cultivation in a greenhouse. Finally, the lesion length on a rice leaf was measured 14 days after inoculation.

2.7. Phytotoxicity test on rice plant

According to the methods we reported previously (Ding et al., 2023; Su et al., 2023), adult rice leaves were sprayed with a solution of compound **B_{16}** (200 or 500 μg/mL) or an equivalent volume of dimethyl sulfoxide. Then, treated rice plants were cultivated in a greenhouse, and photographed 7 days later.

2.8. Statistical analysis.

Each assay was conducted at least three times. Growth curves and bacterial reduction of extracellular results were processed using Origin 2021 (www.originlab.com/2021). Statistical analyses were conducted using SPSS 20.0 (IBM, Armonk, NY, USA) by one-way ANOVA. Data are the mean ± SD.

2.9. Preparation process of intermediates and target molecules

2.9.1. Synthesis of intermediate a

9*H*-carbazole (5.00 g, 29.90 mmol) and KOH (2.01 g, 35.88 mmol) were dissolved in 15 mL of anhydrous dimethylformamide (DMF). Then, 2-(bromomethyl)oxirane (4.92 g, 35.88 mmol) was supplemented, and the mixture then allowed to react for 6 h at 0 °C. Upon complete consumption of 9*H*-carbazole, the mixture was quenched with saturated 40 mL of NH_4Cl solution and extracted by ethyl acetate (3 × 50 mL). The organic layer was washed by saturated NH_4Cl solution, dried with anhydrous Na_2SO_4, and concentrated under a vacuum. Finally, intermediate **a** was further purified by column chromatography on silica gel using petroleum ether and ethyl acetate (180:1, *v/v*) as the eluent.

2.9.2. Synthesis of intermediate b

Briefly, intermediate **a** (22.39 mmol), and 22.39 mmol of K_2CO_3 were dissolved with 30 mL of isopropanol in a 100 mL round-bottomed flask. Then, 22.39 mmol of *tert*-butyl piperazine-1-carboxylate was supplemented, and the mixture then reacted for 6 h at 60 °C. After intermediate **a** had been completely consumed, the solvent was evaporated under reduced pressure. Then, the crude residue was dissolved by

Table 1
In vitro inhibitory effects of compounds **B_1–B_{20}** against *Xoo, Xac* and *Psa*.

Compd.	*Xoo* regression equation	EC_{50} (μg/mL)[a]	*Xac* regression equation	EC_{50} (μg/mL)	*Psa* regression equation	EC_{50} (μg/mL)
B_1	y = 6.4684x − 1.2716	9.07 ± 0.22	y = 5.1174x – 1.9327	3.98 ± 0.11	y = 3.3593x + 1.0391	15.10 ± 0.34
B_2	y = 5.1792x − 0.1507	9.87 ± 0.11	y = 2.6532x + 2.4468	9.17 ± 0.23	y = 3.7600x − 0.9196	37.53 ± 1.16
B_3	y = 4.3257x + 1.1101	7.93 ± 0.47	y = 2.791x + 3.1034	4.78 ± 0.33		>100
B_4	y = 5.2382x − 0.5245	11.34 ± 0.32	y = 4.5397x + 0.9996	7.61 ± 0.63		>100
B_5	y = 5.708x − 2.6925	22.26 ± 0.72	y = 2.199x + 3.2149	6.48 ± 0.52	y = 7.0387x − 6.6301	44.95 ± 2.81
B_6	y = 5.7740x + 3.016	24.45 ± 0.97	y = 2.4149x + 3.0267	6.56 ± 0.89	y = 12.229x + 16.841	61.09 ± 2.37
B_7	y = 11.373x − 12.83	36.96 ± 0.36	y = 2.0158x + 2.1358	26.36 ± 1.38		> 100
B_8		> 100	y = 2.0639x + 2.5883	14.74 ± 2.11		> 100
B_9	y = 4.930x + 1.9856	4.09 ± 0.06	y = 6.5838x + 0.5134	4.80 ± 0.17		> 100
B_{10}	y = 10.070x − 0.9312	3.88 ± 0.01	y = 4.8744x − 3.0000	2.57 ± 0.14	y = 4.0071x + 1.7434	6.50 ± 0.36
B_{11}	y = 11.878x − 2.2635	4.09 ± 0.10	y = 3.0314x + 3.5464	3.02 ± 0.50	y = 0.6553x + 4.5236	5.33 ± 0.59
B_{12}	y = 5.2708x − 1.7229	4.19 ± 0.08	y = 2.5331x + 3.4275	4.18 ± 0.11	y = 3.1672x + 2.4055	6.59 ± 0.06
B_{13}	y = 13.461x − 4.0312	4.69 ± 0.04	y = 3.3087x + 2.9040	4.30 ± 0.31	y = 5.3444x − 0.4114	10.29 ± 0.08
B_{14}	y = 4.6096x + 0.5946	9.03 ± 0.66	y = 2.1058x + 3.0381	8.54 ± 1.88	y = 11.611x − 8.7659	15.33 ± 3.12
B_{15}	y = 15.213x − 7.2434	6.38 ± 0.12	y = 2.9666x + 3.1965	4.05 ± 0.22	y = 5.0128x + 0.0757	9.60 ± 1.07
B_{16}	y = 7.934x + 1.0892	3.11 ± 0.03	y = 2.9281x − 3.5221	3.20 ± 0.08	y = 4.1671x + 2.7119	3.54 ± 0.13
B_{17}	y = 4.3875x + 2.7148	3.32 ± 0.10	y = 5.1203x + 1.459	4.92 ± 0.34	y = 10.202x − 2.6750	5.65 ± 0.84
B_{18}	y = 5.7740x + 3.016	24.45 ± 0.97	y = 4.8225x + 0.3799	9.08 ± 0.55		> 100
B_{19}	y = 11.747x − 1.7541	3.73 ± 0.10	y = 5.3088x + 2.0127	3.65 ± 0.35	y = 1.1340x + 4.1045	6.16 ± 0.70
B_{20}	y = 4.5137x + 2.032	4.55 ± 0.05	y = 4.2307x + 1.8757	5.48 ± 0.19	y = 2.6709x + 2.2109	11.07 ± 0.89
BT[b]	y = 3.6885x − 0.6944	34.98 ± 1.46	y = 3.302x − 1.1895	74.90 ± 3.21		> 100
TC[b]	y = 3.6545x − 1.9426	79.39 ± 3.36	y = 2.822x + 0.0152	58.40 ± 4.8		> 100

[a] EC_{50} values were presented as the mean ± SD (standard deviation) of three independent repetitions. [b] Bactericides bismerthiazol (BT) and thiodiazole copper (TC) were as positive agents.

CH_2Cl_2, washed with water, dried by anhydrous Na_2SO_4, and evaporated under a vacuum. Furthermore, the residue was redissolved in 15 mL of MeOH, acidified using concentrated 2 mL of HCl, and stirred at room temperature for an additional 6 h. Upon full conversion, the solvent was removed and the aqueous phase washed by EtOAc, and NaOH solution (3 mol/L) added dropwise until pH 9 − 10 was reached. Finally, the desired crude product was filtered to obtain intermediate **b** as a yellow oil (4.03 g, yield = 44.0 %).

2.9.3. Synthesis of intermediate c

To a mixture of intermediate **b** (2.00 g, 6.46 mmol) and KOH (0.36 g, 6.46 mmol) in anhydrous DMF (15 mL) was supplemented with 2-(bromomethyl)oxirane (1.33 g, 9.70 mmol) slowly followed by stirring for 6 h at 0 °C. After that, the mixture was quenched by saturated NH_4Cl aqueous solution (15 mL), extracted with EtOAc (3 × 30 mL), dried by anhydrous Na_2SO_4, and evaporated under reduced pressure. The crude residue was then purified further by column chromatography on silica gel using CH_2Cl_2 and CH_3OH (200:1, *v/v*) as the eluent to obtain intermediate **c** as a white solid (1.77 g, yield = 56.4 %).

2.9.4. General synthesis for target compounds B_1–B_{20}

Intermediate **c** (0.30 g, 0.8 mmol), the corresponding amine (1.6 mmol), K_2CO_3 (0.11 g, 0.8 mmol), and isopropanol (10.0 mL) were supplemented to a 50 mL round-bottomed flask, then stirred at 60 °C until intermediate **c** was completely consumed. After that, the solvent was evaporated under reduced pressure, the residue was re-dissolved by water, extracted using EtOAc, dried with anhydrous Na_2SO_4, and concentrated under reduced pressure. The crude product was further purified by column chromatography on silica gel using CH_2Cl_2 and CH_3OH (8:1, *v/v*) as the eluent to afford the expectant title compounds **B_1–B_{20}**.

1-(4-(3-(9*H*-carbazol-9-yl)-2-hydroxypropyl)piperazin-1-yl)-3-(propylamino)propan-2-ol (**B_1**) was a yellow oil (187.17 mg; yield = 53.70 %).

The characterization data (NMR and HRMS) for title molecules **B_2–B_{20}** are described in Supporting Information.

2.9.5. Synthesis of target compounds C_1–C_7

Intermediate **b** (0.23 g, 0.7 mmol), an epoxy intermediate (1.6 mmol), K_2CO_3 (0.15 g, 1.1 mmol), and isopropanol (10.0 mL) were supplemented to a 50 mL oven-dried vial containing a magnetic stirring bar, and stirred for 8 h at 60 °C. When the reaction completed, the mixture was concentrated and further purified by flash chromatography on silica gel (CH_2Cl_2:CH_3OH, 60:1) to afford the target compound **C_1** (yellow oil, yield = 70.3 %).

The characterization data (NMR and HRMS) for the other intermediates and target compounds are described in Supporting Information.

3. Results and discussion

3.1. In vitro bioassay of target compounds and the structure–activity relationship (SAR) analyses

Two series of carbazoles were evaluated for promising antibacterial activity with the turbidimeter test (Table 1). Positive agents were bismerthiazol (BT) and thiodiazole copper (TC) (Qi et al., 2023a; Chu et al., 2023).

Antibacterial tests revealed the excellent activity of compounds **B_1–B_{20}** against all tested bacterial strains. Interestingly, compound **B_{16}** had a prominent effect against *Xoo*, *Xac*, and *Psa*, with EC_{50} values of 3.11, 3.20, and 3.54 μg/mL, respectively. By contrast, intermediate **c** (with substituted piperidine) had different bioactivity depending on the substituent. If the substituent − CH_3 was located on the piperidine ring, the activity of compounds **B_2–B_4** against *Xoo* was in the order 3 − CH_3 (7.93 μg/mL) > 2 − CH_3 (9.87 μg/mL) > 4 − CH_3 (11.34 μg/mL). If the substituents − CH_2CH_3, −$CH(CH_3)_2$, or − $COCH_3$ were located on the piperazine ring, the anti-*Xoo* ability of molecules **B_5–B_7** decreased significantly compared with that of compound **B_{16}**, with EC_{50} values ranging from 22.26 μg/mL to 36.96 μg/mL. However, compound **B_8** with the substituent morpholine had no activity against *Xoo*. Target compounds with benzylamines substituents displayed excellent activity against *Xoo*, with EC_{50} values ranging from 3.11 μg/mL to 24.45 μg/mL. Among them, the substituents containing halogenated atoms had prominent activity against *Xoo*. In particular, compounds substituted with chlorine atoms (as well as their substituted positions and number) had prominent activity against *Xoo* in the order compound **B_{16}** (3 − Cl, 3.11 μg/mL) > **B_{17}** (4 − Cl, 3.32 μg/mL) > **B_{15}** (2 − Cl, 6.38 μg/mL). The activity of molecule **B_{18}** (EC_{50} = 24.45 μg/mL) toward *Xoo* was slightly higher than that of BT (EC_{50} = 34.98 μg/mL). For molecules substituted

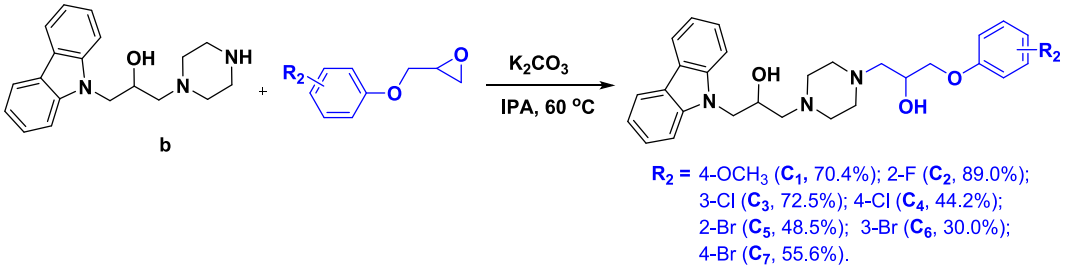

Fig. 3. Synthetic procedure for compounds $\mathbf{C_1}$–$\mathbf{C_7}$.

Table 2
In vitro inhibitory effects of molecules $\mathbf{C_1}$–$\mathbf{C_7}$ against *Xoo*, *Xac* and *Psa*.

Compd.	*Xoo*		*Xac*		*Psa*	
	regression equation	EC_{50} (μg/mL)[a]	regression equation	EC_{50} (μg/mL)	regression equation	EC_{50} (μg/mL)
$\mathbf{C_1}$	y = 30.069x − 34.855	21.16 ± 0.80	y = 2.852x + 2.1975	9.61 ± 0.51	y = 1.3476x + 3.3969	15.47 ± 2.69
$\mathbf{C_2}$	y = 4.6781x + 0.4882	9.21 ± 0.37	y = 3.3399x + 2.1751	7.01 ± 1.62	y = 4.3552x − 0.5733	19.04 ± 0.45
$\mathbf{C_3}$	y = 10.637x − 6.7433	12.71 ± 0.32	y = 3.2233x + 2.4078	6.37 ± 0.52		> 100
$\mathbf{C_4}$	y = 5.1188x + 1.6498	4.51 ± 0.43	y = 4.6822x + 1.9018	4.59 ± 0.28	y = 4.1861x − 0.2995	18.45 ± 0.81
$\mathbf{C_5}$	y = 2.7181x + 2.5200	8.17 ± 0.29	y = 1.2677x + 3.2564	23.74 ± 3.05	y = 1.4877x + 3.0753	19.67 ± 5.16
$\mathbf{C_6}$	y = 4.2917x + 2.1641	4.58 ± 0.12	y = 3.9341x + 1.6069	7.29 ± 0.82		> 100
$\mathbf{C_7}$	y = 5.0397x + 2.0861	3.79 ± 0.17	y = 3.8456x + 1.7646	6.94 ± 0.43	y = 2.8317x − 0.3232	75.33 ± 10.48
BT[b]	y = 3.6885x − 0.6944	34.98 ± 1.46	y = 3.302x − 1.1895	74.90 ± 3.21		> 100
TC[b]	y = 3.6545x − 1.9426	79.39 ± 3.36	y = 2.822x + 0.0152	58.40 ± 4.8		> 100

[a] EC_{50} values were presented as the mean ± SD (standard deviation) of three independent repetitions. [b] Bactericides bismerthiazol (BT) and thiodiazole copper (TC) were as positive agents.

with fluorine atoms, the activity against *Xoo* was in the order $\mathbf{B_{12}}$ (2 − F, 4.19 μg/mL) > $\mathbf{B_{13}}$ (3 − F, 4.69 μg/mL) > $\mathbf{B_{14}}$ (4 − F, 9.03 μg/mL). For activity toward *Xoo*, a similar tendency was discovered to that towards *Xac* and *Psa in vitro*. With respect to activity against *Xac*, compared with control BT (74.90 μg/mL) and TC (58.40 μg/mL), molecules $\mathbf{B_1}$–$\mathbf{B_{20}}$ possessed higher antibacterial ability, with EC_{50} values ranging from 2.57 μg/mL to 26.36 μg/mL. Compared with molecule $\mathbf{B_{16}}$, the 4-OCH_3-benzyl moiety-containing compound $\mathbf{B_{10}}$ and benzyl moiety-containing molecule $\mathbf{B_{11}}$ given EC_{50} values of 2.57 μg/mL and 3.02 μg/mL against *Xac*, and exhibited excellent activity. With regard to *Psa*, the antibacterial activity of target compounds was laudable, and was superior to controls TC (>100 μg/mL) and BT (>100 μg/mL).

Molecule $\mathbf{B_1}$ (with substituted propylamino group) was the optimal active molecule against the three types of pathogenic bacteria. For compounds $\mathbf{B_{19}}$ and $\mathbf{B_{20}}$, similar antibacterial ability against *Xoo*, *Xac*, and *Psa* was observed. Analyses of the bioactivity results of target compounds $\mathbf{B_1}$–$\mathbf{B_{20}}$ against the three types of pathogenic bacteria revealed three main observations. First, the contribution of substituted piperazine and piperidine towards bioactivity was inferior to that of benzylated compounds. Second, if a benzylamine moiety was introduced into the carbazole containing-isopropanolamine, then the antibacterial activity of the title molecules towards the three types of pathogenic bacteria was increased. Third, compounds $\mathbf{B_{19}}$ and $\mathbf{B_{20}}$ (which contained thiophene or furan substituents) had strong activity against *Xoo* (EC_{50} = 3.73 and 4.55 μg/mL), *Xac* (EC_{50} = 3.65 and 5.48 μg/mL) and *Psa* (EC_{50} = 6.16 and 11.07 μg/mL). All title molecules had significant inhibitory effects towards *Xoo* and *Xac*. Compound $\mathbf{B_{16}}$ was most active compound against *Xoo* (EC_{50} = 3.11 μg/mL) and *Psa* (EC_{50} = 3.54 μg/mL). Compound $\mathbf{B_{10}}$ (4-CH_3-benzyl) was the most active compound in terms of anti-*Xac* activity.

In order to probe the effect of benzylamine groups on antibacterial ability, a new series of carbazole derivatives decorated with 3-phenoxypropan-2-ol ($\mathbf{C_1}$–$\mathbf{C_7}$) was designed and synthesized (Fig. 3). The *in vitro* bioassay (Table 2) displayed that the phenoxy-substituted compounds $\mathbf{C_1}$–$\mathbf{C_7}$ exhibited comparative activity against *Xoo* and *Xac* to that of the benzylamine moiety-containing compounds $\mathbf{B_9}$–$\mathbf{B_{20}}$ to afford EC_{50} values of 3–20 μg/mL, but showed reduced potency against *Psa*. Compound $\mathbf{C_7}$ provided optimal EC_{50} values against *Xoo* (EC_{50} = 3.79 μg/mL), and compound $\mathbf{C_4}$ afforded optimal EC_{50} values toward *Xac* (EC_{50} = 4.59 μg/mL), respectively. The position of the substituent on the benzene ring had a significant distinction on antibacterial activity. For instance, the anti-*Xoo* potency of Br atom-containing molecules was in the order *para*- ($\mathbf{C_7}$: 4-bromophenoxy, 3.79 μg/mL) > *meta*- ($\mathbf{C_6}$: 3-bromophenoxy, 4.58 μg/mL) > *ortho*- ($\mathbf{C_5}$: 2-bromophenoxy, 8.17 μg/mL), and had the same trend as that for activity against *Xac*. Taken together, these findings suggested that a 3-phenoxypropan-2-ol moiety could exert antibacterial activity (comparable activity towards *Xoo* and *Xac*, but lower activity toward *Psa*) when compared with that of benzylamine moiety-modified compounds. A benzylamine moiety was vital for exerting broad-spectrum antibacterial activity.

Giving the above-mentioned results, the SAR study was investigated systematically. First, when R_1 was *N*-containing heterocyclic (such as piperazine) or benzylamine groups, the contribution of substituted benzylamine towards bioactivity was superior to substituted piperazine and piperidine moieties. Furthermore, introduction of halogen atom on the benzylamine groups could slightly increase the anti-*Xoo* activity: compound $\mathbf{B_{16}}$ (3 − Cl, 3.11 μg/mL), $\mathbf{B_{17}}$ (4 − Cl, 3.32 μg/mL) > $\mathbf{B_{11}}$ (H, 4.09 μg/mL) and $\mathbf{B_9}$ (4-OCH_3, 4.09 μg/mL). Secondly, when R_1 was replaced as phenols groups, their bioactivities towards *Xoo* and *Xac* were comparable to the corresponding benzylamine-substituted derivatives, but their anti-*Psa* activity was dramatically decreased. By the way, the electron-withdrawing substituent on the benzene ring had a significant enhancement on antibacterial activity. For instance, the anti-*Xoo* potency of molecules was in the order ($\mathbf{C_4}$: 4-chlorine, 4.51 μg/mL), ($\mathbf{C_6}$: 3-bromo, 4.58 μg/mL) and ($\mathbf{C_7}$: 3-bromo, 3.79 μg/mL) > ($\mathbf{C_1}$: 2-bromophenoxy, 21.16 μg/mL). Overall, compound $\mathbf{B_{16}}$ exhibited the optimal bioactivities, especially against *Xoo* (EC_{50} = 3.11 μg/mL), and *Psa* (EC_{50} = 3.54 μg/mL), and was thus selected to evaluate its *in vivo* bioactivity.

3.2. *In vivo* effectiveness against rice bacterial leaf blight and kiwifruit bacterial canker

Taking account of the results of *in vitro* bioassays, compound $\mathbf{B_{16}}$ (with the lowest EC_{50} values of 3.11 and 3.54 μg/mL against *Xoo* and

Table 3
In vivo inhibitory effect of compound $\mathbf{B_{16}}$ against rice bacterial leaf blight at 200 μg/mL.

Treatment	Curative activity			Protective activity		
	Morbidity (%)	Disease index (%)	Control efficiency (%)[b]	Morbidity (%)	Disease index (%)	Control efficiency (%)[b]
B_{16}	100	51.85	38.56 a	100	53.33	35.12 a
TC	100	68.15	19.30c	100	63.70	24.56b
CK[a]	100	84.40		100	84.40	

[a] Negative control. [b]Statistical analysis was conducted by the ANOVA method under the condition of equal variances assumed ($p > 0.05$) and equal variances not assumed ($p < 0.05$). Different lowercase letters indicated the control efficiencies with significant difference among different treatment groups at $p < 0.05$.

Table 4
The inhibitory effect of compound $\mathbf{B_{16}}$ and **TC** toward kiwifruit canker disease at 200 μg/mL.

Treatment	Curative efficiency (%)	Protective efficiency (%)
B_{16}	45.54 ± 6.35 a	67.61 ± 3.73 a
TC	48.32 ± 1.83 a	42.53 ± 4.37 a

[a]Statistical analysis was conducted by ANOVA under the condition of equal variances assumed ($P > 0.05$) and equal variances not assumed ($P < 0.05$). Different uppercase letters indicated the control efficiencies with a significant difference among different treatment groups at $P < 0.05$.

Psa, respectively) was chosen to assess the inhibitory effect for managing RBLB and BCK (Zhang et al., 2023).

Bioassay results (Table 3, Table 4, and Fig. 4) showed that compound $\mathbf{B_{16}}$ had activity against rice BLB at 200 μg/mL. It could protect 35.12 % of samples and cure 38.56 % of samples, and was more efficacious than the commercial TC (19.3 % and 24.56 %, respectively). Compound $\mathbf{B_{16}}$ possessed excellent protective activity against rice BCK at 200 μg/mL (Fig. 5). It could protect 67.61 % of samples [superior to that of TC (42.53 %)] and could cure 45.54 % of samples [superior to that of TC (48.32 %)]. These results suggested that compound $\mathbf{B_{16}}$ could be used to manage bacterial diseases of plants.

3.3. Antibacterial mechanism study

3.3.1. Bacterial growth affected by compound B_{16}

We wished to explore the mechanism of action of molecule $\mathbf{B_{16}}$ against *Xoo* cells. Growth curves were created using compound $\mathbf{B_{16}}$ at 0, 0.78, 1.56, 3.11, 6.22, and 12.44 μg/mL. The growth rate was influenced slightly by compound $\mathbf{B_{16}}$ at doses of 0.78 and 1.56 μg/mL when compared with that of the control sample (Fig. 6). Notably, the growth of *Xoo* cells was obviously inhibited under a compound-$\mathbf{B_{16}}$ concentration of 3.11 μg/mL. In particular, the growth of *Xoo* cells was inhibited completely upon incubation with compound $\mathbf{B_{16}}$ at doses of 6.22 and 12.44 μg/mL. These outcomes suggested that compound $\mathbf{B_{16}}$ possessed a potent inhibitory effect on the growth of *Xoo* cells.

3.3.2. Morphological study

The morphologic changes of *Xoo* cells elicited by treatment with molecule $\mathbf{B_{16}}$ was studied further by SEM using a Nova NanoSEM 450 system (FEI, Hillsboro, OR, USA) (Xie et al., 2023). The surface of control *Xoo* cells possessed an integrated bacterial surface (Fig. 7). Some *Xoo* cells treated with compound $\mathbf{B_{16}}$ (6.22 μg/mL) appeared to have a slightly shrunken and distorted cell surface. However, more serious damage to *Xoo* cells was observed at a dose of 12.44 μg/mL (Fig. 7**c**): malformed, distorted, cracked, and leaking holes appeared on the surface of most *Xoo* cells. Hence, compound $\mathbf{B_{16}}$ had a negative impact on the morphology of *Xoo* cell membranes.

3.3.3. Membrane permeability assay

A membrane-permeability assay was undertaken according to our previously reported methods to verify the functions of *Xoo* cell membranes (Zeng et al., 2023b; Kong et al., 2008; Zhang et al., 2020). Conductivity is increased with changes in the membrane permeability of bacteria. The relative conductivity of a *Xoo*-cell suspension (Fig. 8) increased rapidly after incubation with compound $\mathbf{B_{16}}$ (6.22 and 12.44 μg/mL), especially 1 h after treatment, when the relative conductivity reached 30.82 % and 59.78 %, respectively, much higher than that of the control (20.55 %). The relative conductivity increased persistently during the next 5 h at a compound-$\mathbf{B_{16}}$ concentration of 12.44 μg/mL. These data indicated that molecule $\mathbf{B_{16}}$ could affect the permeability of

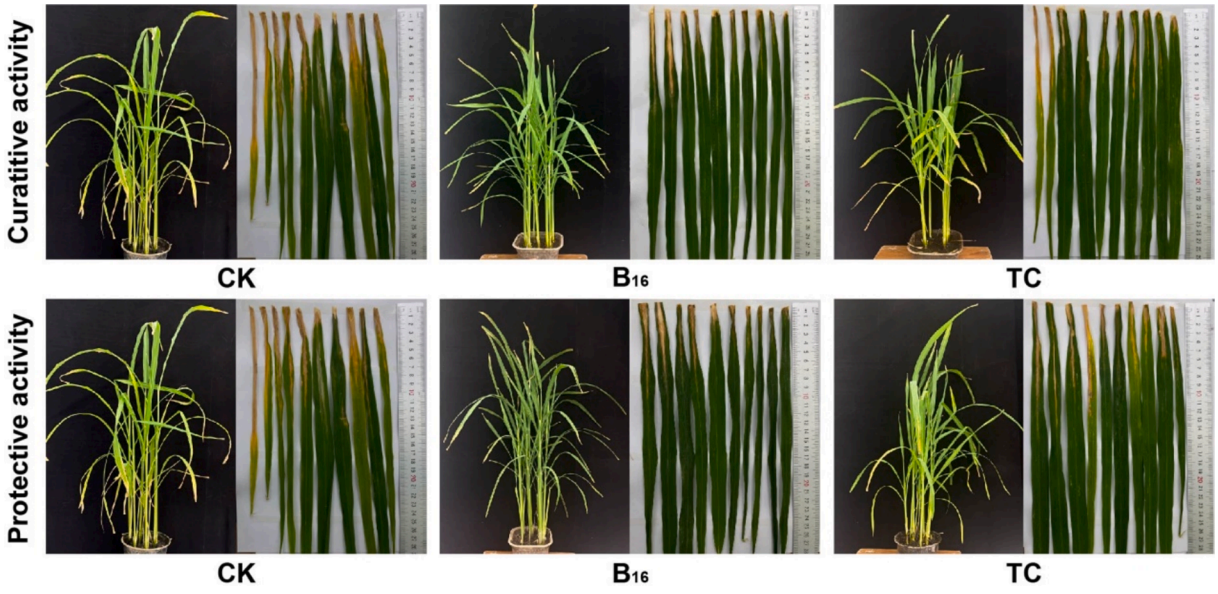

Fig. 4. *In vivo* bioassay of compound $\mathbf{B_{16}}$ towards rice bacterial leaf blight at 200 μg/mL.

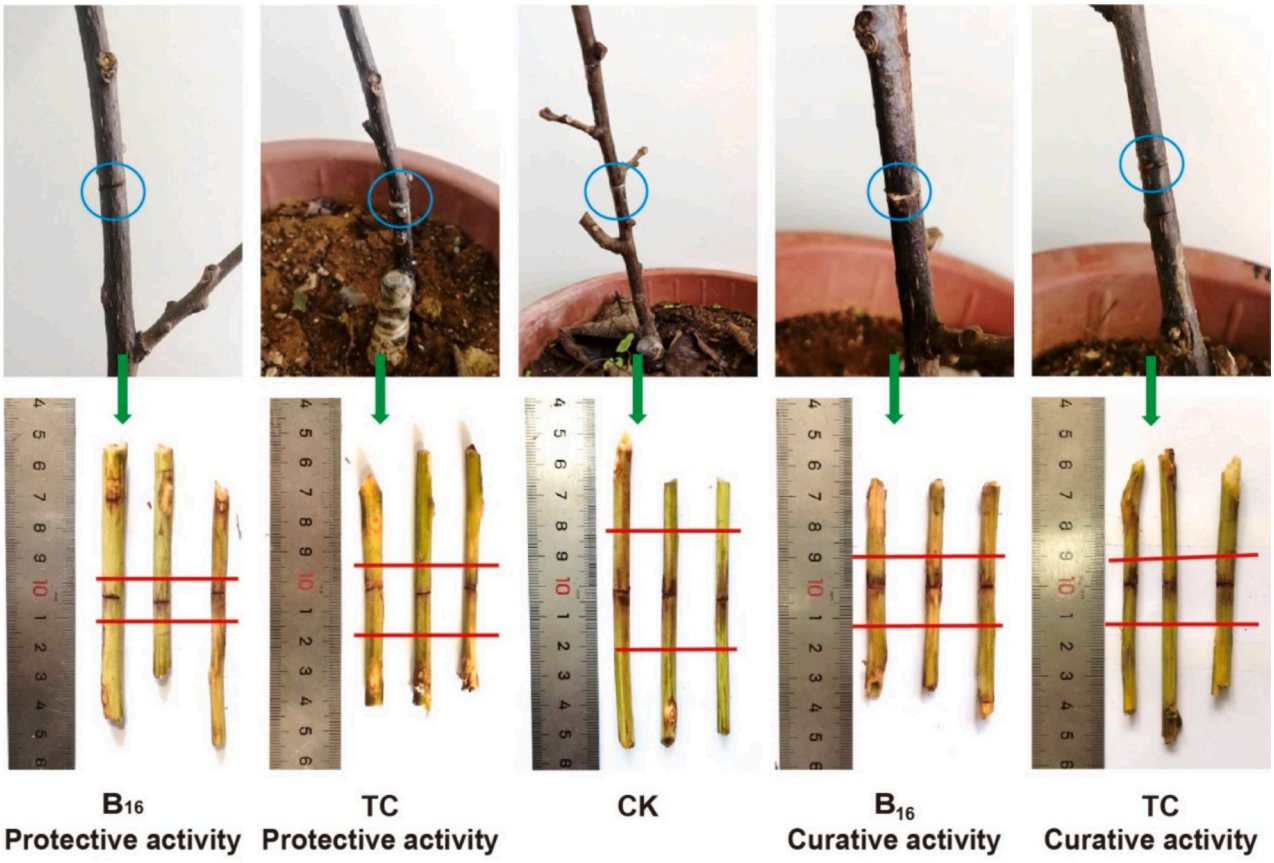

Fig. 5. The inhibitory effect of compound **B_{16}** and **TC** toward kiwifruit bacterial canker under greenhouse conditions at 200 μg/mL.

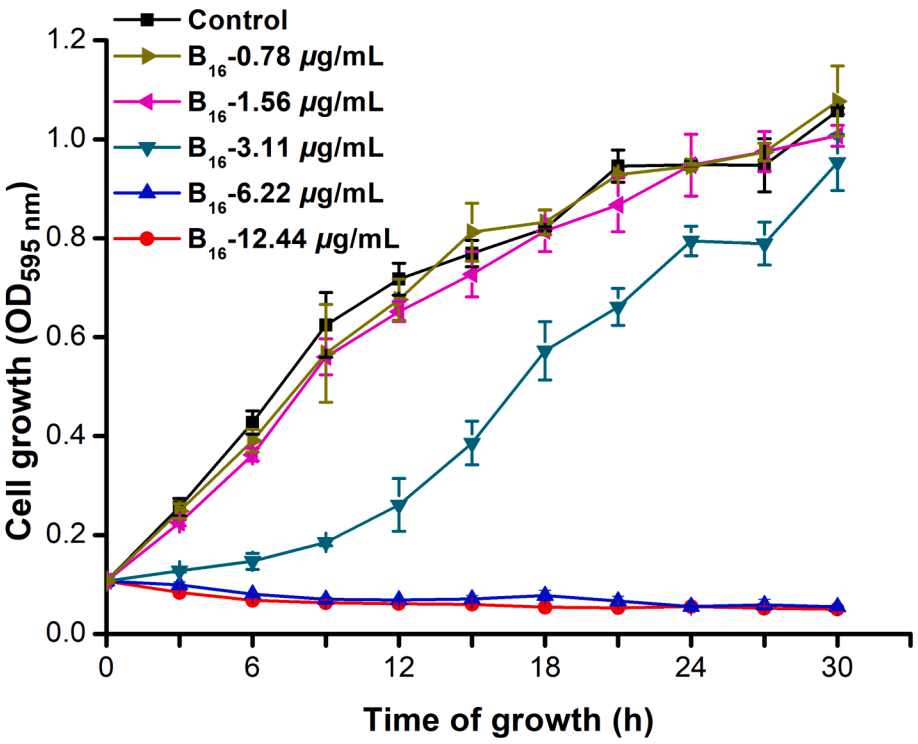

Fig. 6. Growth curve of *Xoo* treated with molecule **B_{16}** at 0, 0.78, 1.56, 3.11, 6.22 and 12.44 μg/mL, respectively.

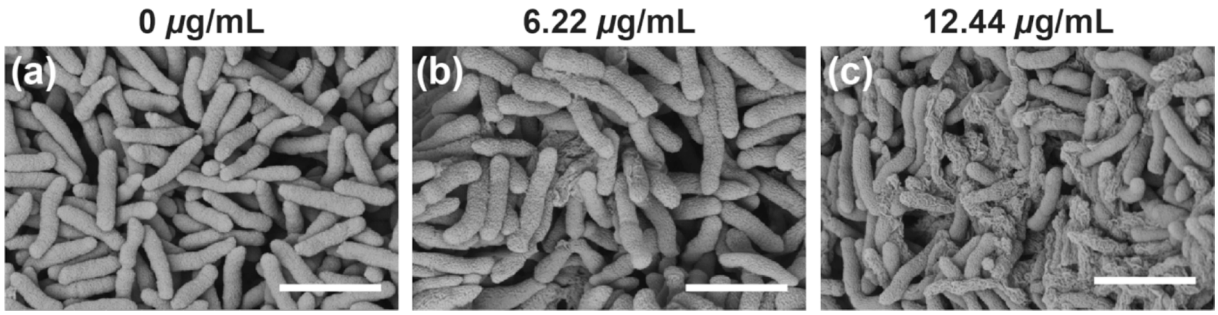

Fig. 7. SEM results of *Xoo* cells after incubating with molecule $\mathbf{B_{16}}$ at 0 μg/mL (**a**), 6.22 μg/mL (**b**) and 12.44 μg/mL (**c**), respectively. Scale bars: 2 μm.

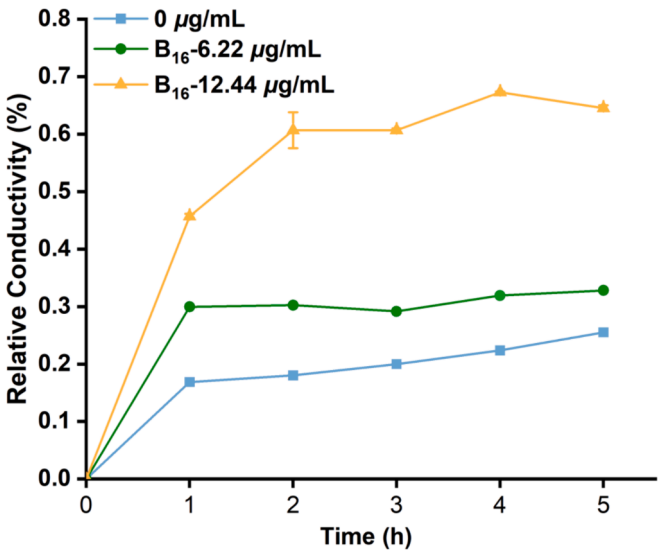

Fig. 8. Relative conductivity of *Xoo* treated with $\mathbf{B_{16}}$ at different concentrations of 0, 6.22 and 12.44 μg/mL, respectively.

the *Xoo*'s membranes significantly, which was in accordance with the morphology data.

3.3.4. PI staining experiment

The dye PI can emit red fluorescence from intercalation with DNA in membrane-damaged cells. PI is used widely to detect cell-membrane permeability and cell viability (Gan et al., 2020; Bownik et al., 2022). The effect on the permeability of *Xoo* cell membranes was observed through measurement of fluorescence intensity with different doses of compound $\mathbf{B_{16}}$ (Fig. 9). Compared with healthy cells (Fig. 9**a**), gradually enhanced red fluorescence (Fig. 9**b–d**) was observed when cells were treated with compound $\mathbf{B_{16}}$. In particular, cells emitted low fluorescence intensity at compound-$\mathbf{B_{16}}$ doses of 12.44 and 24.88 μg/mL. These data demonstrated that target compound $\mathbf{B_{16}}$ could negatively impact the membrane permeability of, and lead to metabolic dysfunction in, *Xoo* cells. These could be key factors for designing molecules with outstanding antibacterial potency.

3.4. Determination of intracellular protein content

The total protein concentration in *Xoo* cells was measured by the Bradford assay to evaluate the damage wrought by compound $\mathbf{B_{16}}$ on bacterial cell membranes (Zhang et al., 2022; kalaivani et al., 2021). The intracellular protein content of *Xoo* cells decreased in a dose-dependent manner with increasing doses of compound $\mathbf{B_{16}}$ (Fig. 10). In particular,

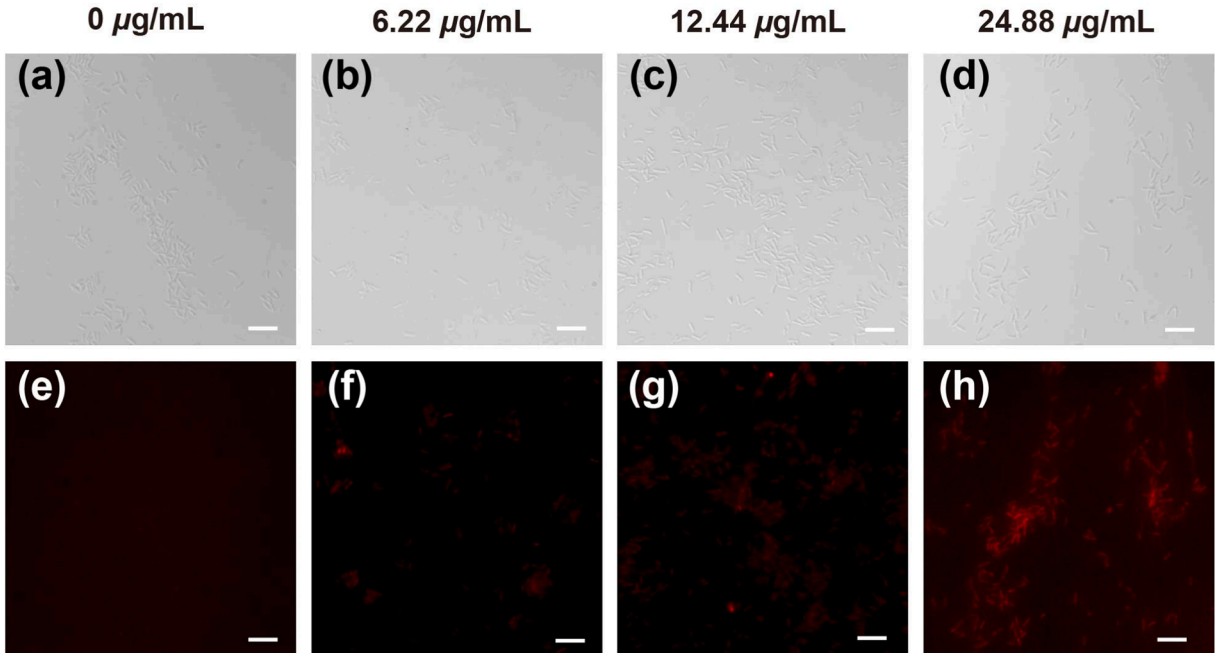

Fig. 9. Morphology of *Xoo* cells staining by PI after incubated with $\mathbf{B_{16}}$ at the dosages of 0, 6.22, 12.44 and 24.88 μg/mL, respectively.

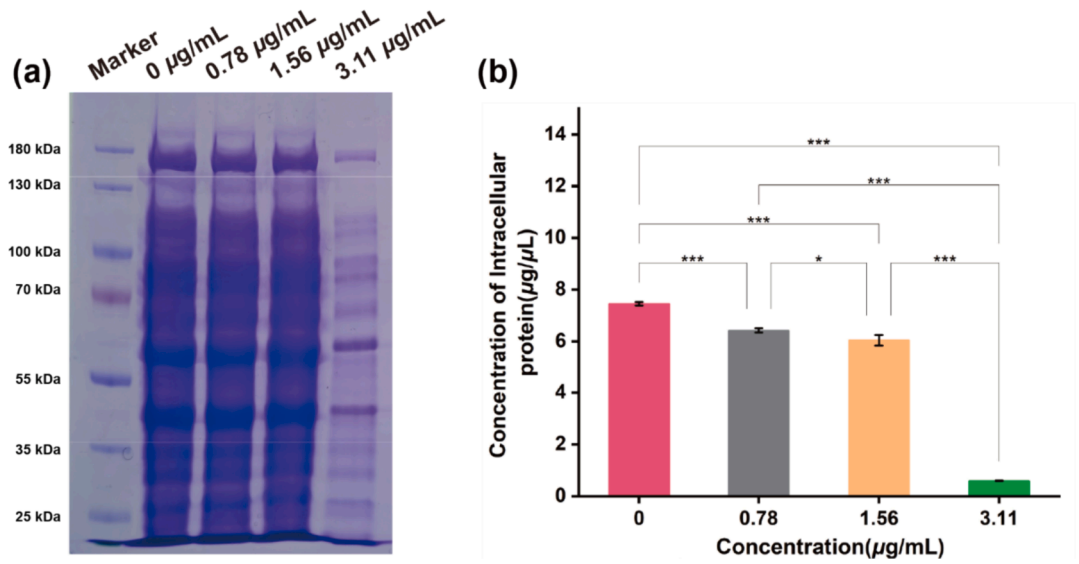

Fig. 10. The intracellular protein content of *Xoo* after incubated with $\mathbf{B_{16}}$ for 14 h at the dosages of 0, 0.78, 1.56 and 3.11 μg/mL, respectively. a) Intracellular proteins content in *Xoo* cell via SDS-PAGE method staining by coomassie blue. b) Corresponding intracellular protein concentration in *Xoo* cells. (For interpretation of the references to colour in this figure legend, the reader is referred to the web version of this article.)

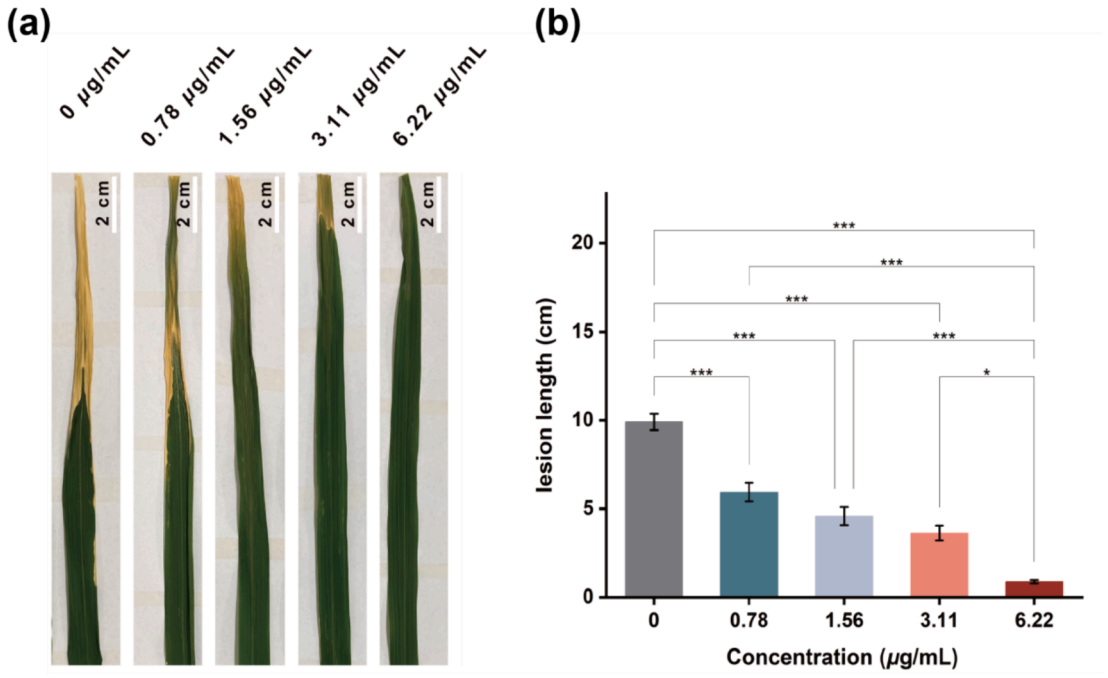

Fig. 11. Pathogenicity analysis triggered by $\mathbf{B_{16}}$ at the dosages of 0, 0.78, 1.56, 3.11 and 6.22 μg/mL on rice plants for 14 days.

the protein content in *Xoo* cell was reduced significantly at a compound-$\mathbf{B_{16}}$ dose of 3.11 μg/mL; the protein content was < 500 μg/mL, which was much lower than that in control cells (>7000 μg/mL). To further investigate the effect of compound $\mathbf{B_{16}}$ on bacterial DNA, the fluorescence titration experiment (Deng et al., 2021; Zhao et al., 2019b) was carried out. The potential interaction between total DNA extracted from *Xoo* and compound $\mathbf{B_{16}}$ was displayed in **Fig. S1**. The results indicated that the fluorescence intensity of compound $\mathbf{B_{16}}$ significantly decreased after the addition of DNA in a dosage-dependent manner. Suggesting that the structure of $\mathbf{B_{16}}$ may be encapsulated in the grooves of the DNA helix, thereby reducing the fluorescence intensity of the carbazole structure.

The above-mentioned results indicated that our designed compound $\mathbf{B_{16}}$ affected the cell membrane function by increasing the permeability of bacterial cell membranes as well as bounding to DNA and further reducing the protein expression. These findings further support the potential of $\mathbf{B_{16}}$ as a promising lead compound for the development of new bactericides.

3.5. *Pathogenicity assays of Xoo on rice*

A pathogenicity test was carried out to ascertain the effect of compound $\mathbf{B_{16}}$ on the pathogenicity of *Xoo* against rice plants (Zeng et al., 2023a; Zhang et al., 2023). The lesion length on rice leaves of the control sample was 10.12 cm at 14 days after inoculation (Fig. 11**a**). Obvious suppression of leaf lesions was observed upon treatment with compound

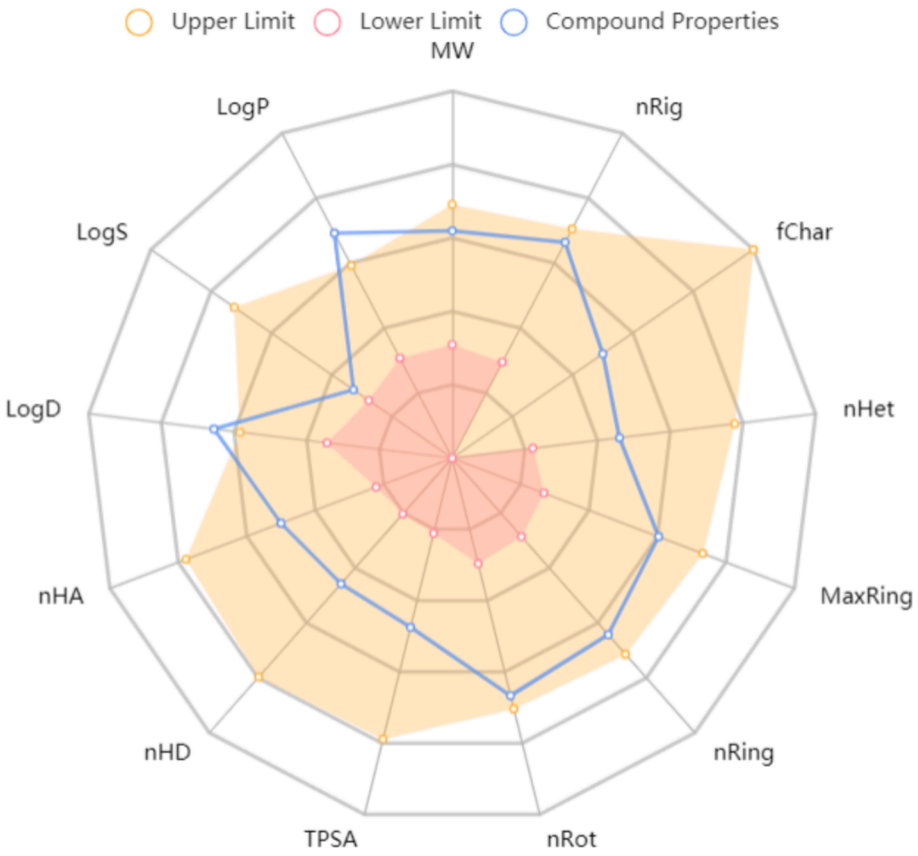

Fig. 12. Physicochemical properties of compound $\mathbf{B_{16}}$.

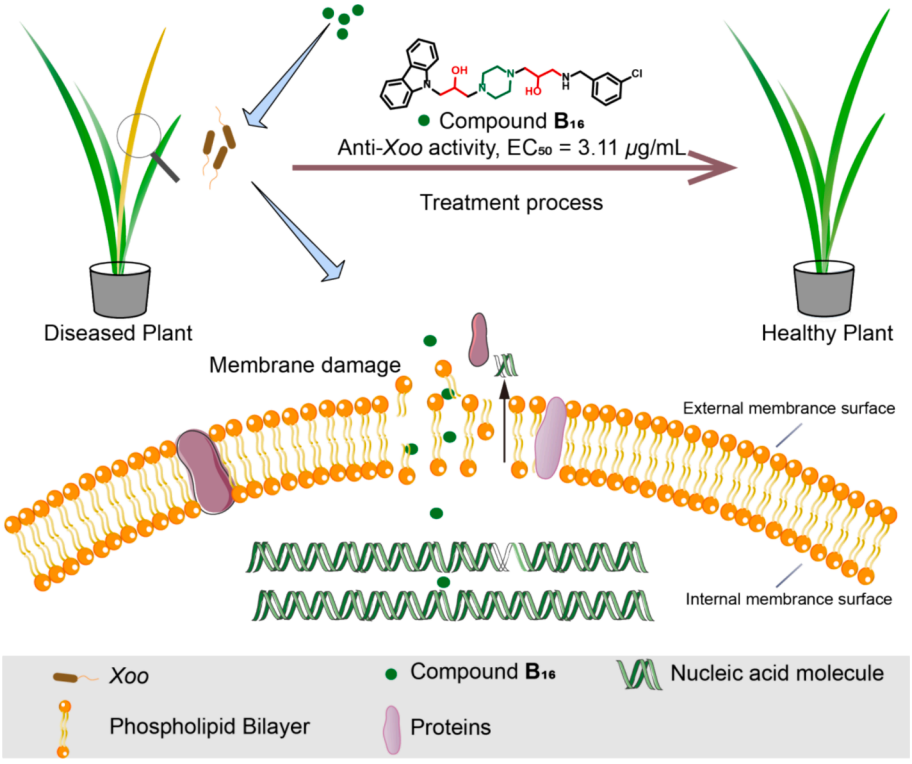

Fig. 13. The hypothesized mechanism of action of compound $\mathbf{B_{16}}$.

B_{16} at > 1.56 μg/mL. Hence, compound **B_{16}** could suppress the pathogenicity of phytopathogenic bacteria.

3.6. The phytotoxicity and in silico 'drug-likeness' evaluation

Finally, the pharmaceutical development of the title compound was assessed, which is the most important step for drug development (Zhou et al., 2022). Toxicity and pharmacokinetic data were used to evaluate if compound **B_{16}** could be a lead compound. Phytotoxicity was evaluated on rice plants: after 7 days of incubation: compound **B_{16}** did not show toxicity towards rice plants (**Fig. S2**). Furthermore, ADMETlab 2.0 (https://admetmesh.scbdd.com/) was employed to ascertain the absorption, distribution, metabolism, excretion, and toxicity (ADMET) and drug-like properties of compound **B_{16}** (Xiong et al., 2021). The physicochemical, ADMET, and drug-like properties of compound **B_{16}** are displayed in Fig. 12 and **Table S2**. Interestingly, molecule **B_{16}** showed acceptable physicochemical, ADMET, and pharmaceutical properties. Especially, compound **B_{16}** had great potential drug-likeness properties, including the Lipinski Rule and Golden Triangle Rule. In summary, our results suggested the excellent pharmacokinetic characteristics and low phytotoxicity of compound **B_{16}**.Fig. 13..

4. Conclusion

A series of 3-(piperazin-1-yl)propan-2-ol-decorated carbazole analogs was synthesized and their antimicrobial ability were evaluated. Bioassay results suggested that the majority of title molecules showed outstanding bactericidal ability towards *Xoo*, *Xac*, and *Psa*, with the optimal EC_{50} values of 3.11 (**B_{16}**), 2.57 (**B_{10}**), and 3.54 (**B_{16}**) μg/mL, respectively, which were superior to commercial BT (30.43, 79.36, and > 100 μg/mL) and TC (82.64, 62.71, and > 100 μg/mL). Furthermore, the SAR analyses indicated that electron-withdrawing group-substituted benzyl amine moieties and the amide groups of compounds **B_1–B_{20}** were the crucial active cores for their outstanding antibacterial effects. *In vivo* bioassays suggested that compound **B_{16}** could control RBLB and protect against BCK. SEM as well as experiments on PI staining and the permeability of cell membranes indicated that compound **B_{16}** had a negative impact on the physiological function and morphology of bacterial cell membranes, changed their permeability, and led to the leakage of intracellular substances, which may be key factors for bacterial death. Additionally, a binding experiment demonstrated that compound **B_{16}** could bind to bacterial DNA, suggesting a potential mechanism by which the compound might inhibit protein synthesis.

This evidence collectively supports the conclusion that compound **B_{16}** could be regarded as a promising lead compound for discovering new bactericides because it targets bacterial cell membranes and potentially interferes with protein synthesis to treat phytopathogenic bacterial infections.

CRediT authorship contribution statement

Si-Yue Ma: Formal analysis, Investigation, Methodology, Writing – original draft. **Ying-Guo Ding:** Formal analysis, Investigation, Methodology. **Xin-Xin Tuo:** Formal analysis, Investigation. **Guo-Qing Wang:** Investigation. **Hong-Wu Liu:** Formal analysis, Investigation. **Jiao Meng:** Formal analysis, Investigation. **Tai-Hong Zhang:** Investigation, Validation. **Li-Wei Liu:** Formal analysis, Investigation. **Pu-Ying Qi:** Investigation. **Xiang Zhou:** Funding acquisition, Investigation, Writing – review & editing. **Song Yang:** Funding acquisition, Methodology, Project administration, Supervision, Writing – review & editing.

Declaration of Competing Interest

The authors declare that they have no known competing financial interests or personal relationships that could have appeared to influence the work reported in this paper.

Acknowledgements

This research was financially supported by National Natural Science Foundation of China (32372610, U23A20201, 32160661, 32202359), National Key Research and Development Program of China (2022YFD1700300), and GZU (Guizhou University) Found for Newly Enrolled Talent (No. 202229).

Appendix A. Supplementary data

Supplementary data to this article can be found online at https://doi.org/10.1016/j.arabjc.2024.105850.

References

Aggarwal, M., Kaur, R., Saha, A., Mudgal, R., Yadav, R., Dash, P.K., Parida, M., Kumar, P., Tomar, S., 2017. Evaluation of antiviral activity of piperazine against chikungunya virus targeting hydrophobic pocket of alphavirus capsid protein. Antivir. Res. 146, 102–111. https://doi.org/10.1016/j.antiviral.2017.08.015.

Ali, Q., Zheng, H., Rao, M.J., Ali, M., Hussain, A., Saleem, M.H., Nehela, Y., Sohail, M.A., Ahmed, A.M., Kubar, K.A., Ali, S., Usman, K., Manghwar, H., Zhou, L., 2022. Advances, limitations, and prospects of biosensing technology for detecting phytopathogenic bacteria. Chemosphere 296, 133773. https://doi.org/10.1016/j.chemosphere.2022.133773.

Ashok, D., Ravi, S., Ganesh, A., Lakshmi, B.V., Adam, S., Murthy, S.D., 2016. Microwave-assisted synthesis and biological evaluation of carbazole-based Chalcones, Aurones and Flavones. Med. Chem. Res. 25, 909–922. https://doi.org/10.1007/s00044-016-1537-7.

Benchlih, S., Esmaeel, Q., Aberkani, K., Tahiri, A., Belabess, Z., Lahlali, R., Barka, E.A., 2023. Modes of action of biocontrol agents and elicitors for sustainable protection against Bacterial Canker of tomato. Microorganisms 11, 726. https://doi.org/10.3390/microorganisms11030726.

Bownik, A., Adamczuk, M., Pawlik-Skowrońska, B., 2022. Behavioral disturbances induced by cyanobacterial oligopeptides microginin-FR1, anabaenopeptin-A and microcystin-LR are associated with neuromotoric and cytotoxic changes in *Brachionus Calyciflorus*. J. Hazard. Mater. 438, 129472 https://doi.org/10.1016/j.jhazmat.2022.129472.

Cauz, A.C., Carretero, G.P., Saraiva, G.K., Park, P., Mortara, L., Cuccovia, I.M., Brocchi, M., Gueiros-Filho, F.J., 2019. Violacein targets the cytoplasmic membrane of bacteria. Acs. Infect. Dis. 5, 539–549. https://doi.org/10.1021/acsinfecdis.8b00245.

Chen, L., Krekels, E.H., Verweij, Paul, E., Buil, J.B., Knibbe, C.A., Brüggemann, R.J., 2020. Pharmacokinetics and pharmacodynamics of posaconazole. Drugs 80, 671–695. https://doi.org/10.1007/s40265-020-01306-y.

Chu, P.L., Feng, Y.M., Long, Z.Q., Xiao, W.L., Ji, J., Zhou, X., Qi, P.Y., Zhang, T.H., Zhang, H., Liu, L.W., Yang, S., 2023. Novel benzothiazole derivatives as potential anti-quorum sensing agents for managing plant bacterial diseases: Synthesis, antibacterial activity assessment, and SAR Study. J. Agr. Food. Chem. 71, 6525–6540. https://doi.org/10.1021/acs.jafc.2c07810.

Deng, H., Zhu, J., Tong, Y., Kong, Y., Tan, C., Wang, M., Wan, M., Meng, X., 2021. Antibacterial characteristics and mechanisms of action of *Aronia melanocarpa* anthocyanins against *Escherichia coli*. LWT 150, 112018. https://doi.org/10.1016/j.lwt.2021.112018.

Ding, Y.G., Chen, A.Q., Wang, N., Long, Z.Q., Liu, H.W., Xie, J., Liu, S.T., Qi, P.Y., Zhou, X., Liu, L.W., Yang, S., 2023. Discovery of novel 3-(piperazin-1-yl)propan-2-ol decorated carbazole derivatives as new membrane-targeting antibacterial agents. Arab. J. Chem. 16, 104991 https://doi.org/10.1016/j.arabjc.2023.104991.

Fang, H., Chen, Z., Hua, X., Liu, W., Xue, C., Liu, Y., Zhu, X., Yuan, M., Cheng, S., Wang, B., Ru, J., Bazhanau, D., Cui, Y., 2022. Synthesis and biological activity of amide derivatives derived from natural product Waltherione f. Med. Chem. Res. 31, 485–496. https://doi.org/10.1007/s00044-022-02852-8.

Gan, B.-H., Cai, X., Javor, S., Köhler, T., Reymond, J.-L., 2020. Synergistic effect of propidium iodide and small molecule antibiotics with the antimicrobial peptide dendrimer G3KL against gram-negative bacteria. Molecules 25, 5643. https://doi.org/10.3390/molecules25235643.

Gerits, E., Blommaert, E., Lippell, A., O'Neill, A.J., Weytjens, B., De Maeyer, D., Fierro, A. C., Marchal, K., Marchand, A., Chaltin, P., Spincemaille, P., De Brucker, K., Thevissen, K., Cammue, B.P.A., Swings, T., Liebens, V., Fauvart, M., Verstraeten, N., Michiels, J., 2016. Elucidation of the Mode of Action of a New Antibacterial Compound Active against Staphylococcus aureus and Pseudomonas aeruginosa. PLOS ONE 11 (5), e0155139.

Hasheminejad, N., Khodaiyan, F., Safari, M., 2019. Improving the antifungal activity of clove essential oil encapsulated by chitosan nanoparticles. Food. Chem. 275, 113–122. https://doi.org/10.1016/j.foodchem.2018.09.085.

Huang, X., Liu, H.W., Long, Z.Q., Li, Z.X., Zhu, J.J., Wang, P.Y., Qi, P.Y., Liu, L.W., Yang, S., 2021. Rational optimization of 1,2,3-triazole-tailored carbazoles as prospective antibacterial alternatives with significant in vivo control efficiency and unique mode of action. J. Agr. Food. Chem. 69, 4615–4627. https://doi.org/10.1021/acs.jafc.1c00707.

Hurley, K.A., Heinrich, V.A., Hershfield, J.R., Demons, S.T., Weibel, D.B., 2015. Membrane-targeting DCAP analogues with broad-spectrum antibiotic activity

against pathogenic bacteria. Acs. Med. Chem. Lett. 6, 466–471. https://doi.org/10.1021/acsmedchemlett.5b00024.
Issa, S., Prandina, A., Bedel, N., Rongved, P., Yous, S., Le Borgne, M., Bouaziz, Z., 2019. Carbazole scaffolds in cancer therapy: A review from 2012 to 2018. J. Enzym. Inhib. Med. Ch. 34, 1321–1346. https://doi.org/10.1080/14756366.2019.1640692.
Jain, A., Chaudhary, J., Khaira, H., Chopra, B., Dhingra, A., 2020. Piperazine: A promising scaffold with analgesic and anti-inflammatory potential. Drug. Res. 71, 62–72. https://doi.org/10.1055/a-1323-2813.
Ji, J., Shao, W.B., Chu, P.L., Xiang, H.M., Qi, P.Y., Zhou, X., Wang, P.Y., Yang, S., 2022. 1,3,4-oxadiazole derivatives as plant activators for controlling plant viral diseases: Preparation and assessment of the effect of Auxiliaries. J. Agr. Food. Chem. 70, 7929–7940. https://doi.org/10.1021/acs.jafc.2c01988.
Jin, P., Wang, Y., Tan, Z., Liu, W., Miao, W., 2020. Antibacterial activity and rice-induced resistance, mediated by C_{15}surfactin A, in controlling rice disease caused by *Xanthomonas oryzae* pv. *oryzae*. Pestic. Biochem. Phys. 169, 104669 https://doi.org/10.1016/j.pestbp.2020.104669.
Kalaivani, K., Maruthi-Kalaiselvi, M., Senthil-Nathan, S., 2021. Seed treatment and foliar application of methyl salicylate (MeSA) as a defense mechanism in rice plants against the pathogenic bacterium, *Xanthomonas oryzae* pv. *oryzae*. Pestic. Biochem. Phys. 171, 104718 https://doi.org/10.1016/j.pestbp.2020.104718.
Keskin, D., Sadri, S., Eskazan, A.E., 2016. Dasatinib for the treatment of chronic myeloid leukemia: Patient selection and special considerations. Drug. Des. Dev. Ther. 10, 3355–3361. https://doi.org/10.2147/DDDT.S85050.
Kong, M., Chen, X.G., Liu, C.S., Liu, C.G., Meng, X.H., Yu, L.J., 2008. Antibacterial mechanism of chitosan microspheres in a solid dispersing system against *E. Coli*. Colloid. Surface. b. 65, 197–202. https://doi.org/10.1016/j.colsurfb.2008.04.003.
Li, Z.X., Yang, B.X., Ding, Y., Meng, J., Hu, J.H., Zhou, X., Liu, L.W., Wu, Z.B., Yang, S., 2023. Insights into a class of natural eugenol and its optimized derivatives as potential tobacco mosaic virus helicase inhibitors by structure-based Virtual Screening. Int. J. Biol. Macromol. 248, 125892 https://doi.org/10.1016/j.ijbiomac.2023.125892.
Lin, S., Liu, J., Li, H., Liu, Y., Chen, Y., Luo, J., Liu, S., 2020. Development of highly potent carbazole amphiphiles as membrane-targeting antimicrobials for treating gram-positive bacterial infections. J. Med. Chem. 63, 9284–9299. https://doi.org/10.1021/acs.jmedchem.0c00433.
Lu, H., Shen, Z., Xu, Y., Wu, L., Hu, D., Song, R., Song, B., 2023. Immune Mechanism of Ethylicin-Induced Resistance to *Xanthomonas oryzae* pv. *oryzae* in Rice. J. Agr. Food. Chem. 71, 288–299. https://doi.org/10.1021/acs.jafc.2c07385.
Lyu, Q., Bai, K., Kan, Y., Jiang, N., Thapa, S.P., Coaker, G., Li, J., Luo, L., 2019. Variation in Streptomycin Resistance Mechanisms in *Clavibacter michiganensis*. Phytopathology 109, 1849–1858. https://doi.org/10.1094/PHYTO-05-19-0152-R.
Ma, Y., Wang, Y.R., He, Y.H., Ding, Y.Y., An, J.X., Zhang, Z.J., Zhao, W.B., Hu, Y.M., Liu, Y.Q., 2022. Drug repurposing strategy part 1: From approved drugs to agribactericides leads. J. Antibiot. 76, 27–51. https://doi.org/10.1038/s41429-022-00574-y.
Merzouki, O., Arrousse, N., El Barnossi, A., Ech-chihbi, E., Fernine, Y., Iraqi Housseini, A., Rais, Z., Taleb, M., 2023. Eco-friendly synthesis, characterization, *in-silico* ADMET and molecular docking analysis of novel carbazole derivatives as antibacterial and antifungal agents. J. Mol. Struct. 1271, 133966 https://doi.org/10.1016/j.molstruc.2022.133966.
Naclerio, G.A., Sintim, H.O., 2020. Multiple ways to kill bacteria via inhibiting novel cell wall or membrane targets. Future. Med. Chem. 12, 1253–1279. https://doi.org/10.4155/fmc-2020-0046.
Perrine-Walker, F., Le, K., 2020. Propidium iodide enabled live imaging of pasteuria sp.-pratylenchus zeae infection studies under fluorescence microscopy. Protoplasma 258, 279–287. https://doi.org/10.1007/s00709-020-01567-0.
Qi, P.Y., Wang, N., Zhang, T.H., Feng, Y.M., Zhou, X., Zeng, D., Meng, J., Liu, L.W., Jin, L.H., Yang, S., 2023a. Anti-virulence strategy of novel dehydroabietic acid derivatives: Design, synthesis, and antibacterial evaluation. Int. J. Mol. Sci. 24, 2897. https://doi.org/10.3390/ijms24032897.
Qi, P.Y., Zhang, T.H., Wang, N., Feng, Y.M., Zeng, D., Shao, W.B., Meng, J., Liu, L.W., Jin, L.H., Zhang, H., Zhou, X., Yang, S., 2023b. Natural products-based botanical bactericides discovery: Novel abietic acid derivatives as anti-virulence agents for plant disease management. J. Agric. Food. Chem. 71, 5463–5475. https://doi.org/10.1021/acs.jafc.2c08392.
Ran, Q.Q., Tao, L.L., Zhou, X., Li, S.M., Yuan, C.M., Yang, S., Zhou, K., 2023. Geranylation of chalcones by a fungal aromatic prenyltransferase. J. Agric. Food. Chem 71, 4675–4682. https://doi.org/10.1021/acs.jafc.2c08743.
Rego, A., Ribeiro, A., Côrte-Real, M., Chaves, S.R., 2022. Monitoring yeast regulated cell death: Trespassing the point of no return to loss of plasma membrane integrity. Apoptosis 27, 778–786. https://doi.org/10.1007/s10495-022-01748-7.
Shao, L.H., Zhao, S., Yang, S., Zhou, X., Li, Y., Li, C.P., Chen, D.P., Li, Z.R., Ouyang, G.P., Wang, Z.C., 2023. Design, synthesis, antibacterial evaluation, three-dimensional quantitative structure–activity relationship, and mechanism of novel Quinazolinone derivatives. J. Agric. Food. Chem. 71, 3939–3949. https://doi.org/10.1021/acs.jafc.2c07264.
Shaquiquzzaman, M., Verma, G., Marella, A., Akhter, M., Akhtar, W., Khan, M.F., Tasneem, S., Alam, M.M., 2015. Piperazine scaffold: A remarkable tool in generation of diverse pharmacological agents. Eur. J. Med. Chem. 102, 487–529. https://doi.org/10.1016/j.ejmech.2015.07.026.
Su, S.S., Liu, H.W., Zhang, J.R., Qi, P.Y., Ding, Y., Ling, Z., Yang, L.L., Liu, L.W., Zhou, X., Yang, S., 2023. Discovery and structure–activity relationship studies of novel tetrahydro-β-carboline derivatives as apoptosis initiators for treating bacterial infections1. J. Integr. Agric. https://doi.org/10.1016/j.jia.2023.05.031.
Vignaroli, G., Iovenitti, G., Zamperini, C., Coniglio, F., Calandro, P., Molinari, A., Fallacara, A.L., Sartucci, A., Calgani, A., Colecchia, D., Mancini, A., Festuccia, C., Dreassi, E., Valoti, M., Musumeci, F., Chiariello, M., Angelucci, A., Botta, M., Schenone, S., 2017. Prodrugs of Pyrazolo[3,4-d]pyrimidines: From Library Synthesis to Evaluation as Potential Anticancer Agents in an Orthotopic Glioblastoma Model. J. Med. Chem. 60, 6305–6320. https://doi.org/10.1021/acs.jmedchem.7b00637.
Wang, F., Liu, H.W., Zhang, L., Liu, S.T., Zhang, J.R., Zhou, X., Wang, P.Y., Yang, S., 2022. Discovery of novel rost-4-ene derivatives as potential plant activators for preventing phytopathogenic bacterial infection: Design, synthesis and biological studies. Pest. Manag. Sci. 78, 3404–3415. https://doi.org/10.1002/ps.6981.
Xiang, H.M., Meng, J., Shao, W.B., Zeng, D., Ji, J., Wang, P.Y., Zhou, X., Qi, P.Y., Liu, L.W., Yang, S., 2023. Plant protein-based self-assembling core–shell nanocarrier for effectively controlling plant viruses: Evidence for nanoparticle delivery behavior, Plant Growth Promotion, and plant resistance induction. Chem. Eng. J. 464, 142432 https://doi.org/10.1016/j.cej.2023.142432.
Xiao, W.L., Wang, N., Yang, L.L., Feng, Y.M., Chu, P.L., Zhang, J.J., Liu, S.S., Shao, W.B., Zhou, X., Liu, L.W., Yang, S., 2023. Exploiting natural maltol for synthesis of novel Hydroxypyridone derivatives as promising anti-virulence agents in bactericides discovery. J. Agr. Food. Chem. 71, 6603–6616. https://doi.org/10.1021/acs.jafc.3c00465.
Xie, J., Long, Z.Q., Chen, A.Q., Ding, Y.G., Liu, S.T., Zhou, X., Liu, L.W., Yang, S., 2023. Novel sulfonamide derivatives containing a piperidine moiety as new bactericide leads for managing plant bacterial diseases. Int. J. Mol. Sci. 24, 5861. https://doi.org/10.3390/ijms24065861.
Xiong, G.L., Wu, Z.X., Yi, J.C., Fu, L., Yang, Z.J., Hsieh, C.Y., Yin, M.Z., Zeng, X.X., Wu, C.K., Lu, A.P., Chen, X., Hou, T.J., Cao, D.S., 2021. ADMETlab 2.0: An integrated online platform for accurate and comprehensive predictions of ADMET properties. Nucleic Acids Res. 49 https://doi.org/10.1093/nar/gkab255.
Xue, Y.J., Li, M.Y., Jin, X.J., Zheng, C.J., Piao, H.R., 2021. Design, synthesis and evaluation of carbazole derivatives as potential antimicrobial agents. Journal of Enzyme Inhibition and Medicinal Chemistry 36 (1), 296–307. https://doi.org/10.1080/14756366.2020.1850713.
Yang, J.H., Wang, X.Y., Zhou, Y.P., Lu, R., Chen, C.H., Zhang, M.H., Cheng, Y.Y., Morris-Natschke, S.L., Lee, K.-H., Wang, Y.-S., 2019. Carbazole alkaloids from *Clausena anisum-olens*: Isolation, characterization, and Anti-HIV Evaluation. Molecules 25, 99. https://doi.org/10.3390/molecules25010099.
Yang, J., Ye, H.J., Xiang, H.M., Zhou, X., Wang, P.Y., Liu, S.S., Yang, B.Y., Yang, H.B., Liu, L.W., Yang, S., 2023. Photo-stimuli smart supramolecular self-assembly of azobenzene/β-cyclodextrin inclusion complex for controlling plant bacterial diseases. Adv. Funct. Mater. 33 https://doi.org/10.1002/adfm.202303206.
Yang, T., Zhang, T., Zhou, X., Wang, P.Y., Gan, J.H., Song, B.A., Yang, S., Yang, C.-G., 2021. Dysregulation of CLPP by small-molecule activators used against *Xanthomonas oryzae* pv. *oryzae* infections. J. Agr. Food. Chem. 69, 7545–7553. https://doi.org/10.1021/acs.jafc.1c01470.
Zeng, C.M., Avula, S.R., Meng, J.P., Zhou, C.H., 2023a. Synthesis and biological evaluation of piperazine hybridized coumarin indolylcyanoenones with antibacterial potential. Molecules 28, 2511. https://doi.org/10.3390/molecules28062511.
Zeng, D., Liu, S.S., Shao, W.B., Zhang, T.H., Qi, P.Y., Liu, H.W., Zhou, X., Liu, L.W., Zhang, H., Yang, S., 2023b. New inspiration of 1,3,4-oxadiazole agrochemical candidates: Manipulation of a type III secretion system-induced bacterial starvation mechanism to prevent plant bacterial diseases. J. Agr. Food. Chem. 71, 2804–2816. https://doi.org/10.1021/acs.jafc.2c07486.
Zeng, D.L., Tian, Z.X., Rao, Y.C., Dong, G.J., Yang, Y.L., Huang, L.C., Leng, Y.J., Xu, J., Sun, C., Zhang, G.H., Hu, J., Zhu, L., Gao, Z.Y., Hu, X.M., Guo, L.B., Xiong, G.S., Wang, Y.H., Li, J.Y., Qian, Q., 2017. Rational design of high-yield and superior-quality rice. Nat. Plants 3. https://doi.org/10.1038/nplants.2017.31.
Zhang, J.J., Feng, Y.M., Zhang, J.R., Xiao, W.L., Liu, S.S., Zhou, X., Zhang, H., Wang, P.Y., Liu, L.W., Yang, S., 2023. Resistance-driven innovations in the discovery of bactericides: Novel triclosan derivatives decorating isopropanolamine moiety as promising anti-biofilm agents against destructive plant bacterial diseases. Pest Manag. Sci. 79, 2443–2455. https://doi.org/10.1002/ps.7419.
Zhang, J.T., Li, Y.C., Zhang, X., Zhou, B., Sun, T., Li, X.P., 2020. Physicochemical properties and antibacterial mechanism of TP microcapsules/LZM-PVA gradual sustained-release composite coatings. Prog. Org. Coat. 146, 105740 https://doi.org/10.1016/j.porgcoat.2020.105740.
Zhang, A., Song, R., Wang, R., Li, H., Hu, D., Song, B., 2022. Synthesis and Antibacterial Activities of 2-Oxo-N-phenylacetamide Derivatives Containing a Dissulfone Moiety Target on Clp. J. Agr. Food. Chem. 70, 9356–9366. https://doi.org/10.1038/nplants.2017.31.
Zhao, Y. L., Huang, X., Liu, L. W., Wang, P. Y., Long, Q. S., Tao, Q. Q., Li, Z., & Yang, S., 2019. Identification of Racemic and Chiral Carbazole Derivatives Containing an Isopropanolamine Linker as Prospective Surrogates against Plant Pathogenic Bacteria: *In Vitro* and *In Vivo* Assays and Quantitative Proteomics. J. Agric. Food Chem., 67(26), 7512–7525. doi: 10.1021/acs.jafc.9b02036.
Zhao, Y.L., Huang, X., Liu, L.W., Wang, P.Y., Long, Q.S., Tao, Q.Q., Li, Z., Yang, S., 2019b. Identification of racemic and chiral carbazole derivatives containing an isopropanolamine linker as prospective surrogates against plant pathogenic bacteria: in vitro and in vivo assays and quantitative proteomics. J. Agr. Food. Chem. 67, 7512–7525. https://doi.org/10.1021/acs.jafc.9b02036.
Zhou, X., Fu, Y.H., Zou, Y.Y., Meng, J., OuYang, G.P., Ge, Q.S., Wang, Z.C., 2022. Discovery of simple diacylhydrazine-functionalized cinnamic acid derivatives as potential microtubule stabilizers. Int. J. Mol. Sci. 23, 12365. https://doi.org/10.3390/ijms232012365.
Zhou, H., Li, M., Liu, H., Liu, Z., Wang, X., Wang, S., 2023. Design, synthesis, and biological evaluation of piperazine derivatives involved in the 5-HT 1A R/BDNF/PKA pathway. Journal of Enzyme Inhibition and Medicinal Chemistry 39 (1). https://doi.org/10.1080/14756366.2023.2286183.